PART I: THEORETICAL BACKGROUND, NUMERICAL AND EXPERIMENTAL ADVANCED STUDIES

EROSION OF INTERACTIVE BUCKLING LOAD OF THIN-WALLED STEEL BAR MEMBERS: CONTRIBUTION OF "TIMISOARA SCHOOL"

DAN DUBINA[1, 2], VIOREL UNGUREANU[1, 2]

Abstract. The paper presents a summary of the activity and research achievements of the Romanian researchers of *Timisoara School* in the field of stability of cold-formed steel members. Both, fundamental theory and applied instability contributions are focussed. Post-critical theory of elastic structures, the analysis of stable and unstable components of bifurcation load, coupling of bifurcations modes (e.g. mod interaction), erosion of critical load are the topics in which the theoretical contributions of *Timisoara School* are significant. Present paper focuses the mode interaction problems of thin-walled steel bar members only, integrating some relevant results obtained by the authors through a state-of-art review.

Key words: erosion, critical load, interactive buckling, ECBL approach, bar members.

1. INTRODUCTION

In the case of an ideal structure, the theoretical equilibrium *bifurcation point* and corresponding load, N_{cr}, are obtained at the intersection of the pre-critical (primary) force-displacement curve with the post-critical (secondary) curve. For a real structure, affected by a generic imperfection the bifurcation point does not appear anymore and, instead, the equilibrium *limit point* is the one characterizing the ultimate capacity, N_u, of the structure. The difference between N_{cr} and N_u represents the *Erosion of the Critical Bifurcation Load (ECBL)*, due to the imperfections. This model applies in the *instability mode interaction*. The meaning of *mode interaction* inherently refers to the erosion of critical bifurcation load in case of interaction of two (or more) buckling modes associated with the same, or nearly the same, critical load. The theoretical and experimental studies and the contributions of *Timisoara School* to this topic along more than 30 years are relevant, being recognised by the scientific community in the field [10].

[1] "Politehnica" University of Timisoara, Civil Engineering Faculty, Department of Steel Structures and Structural Mechanics, Ioan Curea 1, 300224, Timisoara, Romania

[2] The Romanian Academy, Timisoara Branch, Laboratory of Steel Structures, Mihai Viteazu 24, 300223, Timisoara, Romania

Ro. J. Techn. Sci. – Appl. Mechanics, Volume 59, N^{os} 1–2, P. 9–137, Bucharest, 2014

As a prove, in October 1982, the First Session of the *Third SSRC International Colloquium of Stability* of Steel Structures was organised in Timisoara. Ten years later, the First *International Conferences on Coupled Instabilities in Metal Structures – CIM'92,* took place in Timisoara on October 10-12, 1992. A number of 61 contributions prepared by 60 authors of 19 countries have been published in a Special Issue of Thin-walled Structures journal, with J. Rondal, D. Dubina and V. Gioncu as Guest Editors [1]. At the second conference, CIMS'96, held in Liege, on September 5-7, 1996, 166 authors from 23 countries presented 62 contributions published in a volume of 596 pages, edited by the same team [2]; and the series continues with the next CIMS,2000 in Lisbon, 2004 in Rome, 2008 in Sydney, 2012 in Glasgow, the being planned to be held in 2016 in Baltimore.

In 1997, the series of International Colloquia dedicated to Stability of Steel Structures promoted by Structural Stability research Council of USA through travelling Sessions (e.g. as the one held in 1982 in Timisoara), extended the topic area and became *International Colloquium on Stability and Ductility of Steel Structures* (SDSS). First SDDS was organized in Nagoya, in august 1997; the next, SDSS'99, has been organised in 9-11 of September 1999 in Timisoara, by the Politehnica University of Timisoara, Technical University of Budapest and Romanian Academy – Timisoara Branch in co-operation with Structural Stability Research Council (USA) and European Convention for Constructional Steelwork [5] and. In 2016, Politehnica University of Timisoara will organise the next edition of SDSS colloquium. In parallel with this events, the *advanced courses* focusing selected structural stability topics, organized by International Centre of Mechanical Sciences-CIMS, in Udine, Italy , with the contribution of outstanding teams of outstanding international lectures , including t representatives of *Timisoara School*, must be emphasized i.e.

– *Coupled Instabilities in Metal Structures. Theory and Practical Aspects* [6] in October 1996;

– *Light gauge metal structures. Recent advances* [7] in June 2002;

– *Phenomenological and mathematical modelling of coupled instabilities* [8] in October 2003.

Continuing the line, in 2004 a Special Issue of Thin Walled Structures journal entitled *Cold Formed Structures: Recent – Research Advances in Central and Eastern Europe* has been published, under the coordination of Professor Dubina [9].

On the following, this *review paper*, focuses the mode interaction problems of thin-walled steel bar members, presenting the theoretical background of ECBL method – *Erosion of Critical Buckling Load* , and selected results obtained with this method. ECBL is a creation of *Timisoara School* of Stability of Steel Structures.

2. PHENOMENON OF MODE INTERACTION

In the case of an ideal structure, the theoretical equilibrium *bifurcation point* and corresponding load, N_{cr}, are observed at the intersection of the pre-critical (primary) force-displacement curve with the post-critical (secondary) curve (see Fig. 1). To evaluate the behaviour of a slender structure, which might loss its stability, needs for the control by design the three characteristic ranges of load-deformation:

- Pre-critical range, i.e. $N \in (0, N_{cr}]$, defining the domain of *structural stability*;
- Critical point (bifurcation of equilibrium);
- Post-critical range, e.g. $N > N_{cr}$, the *structural instability* domain.

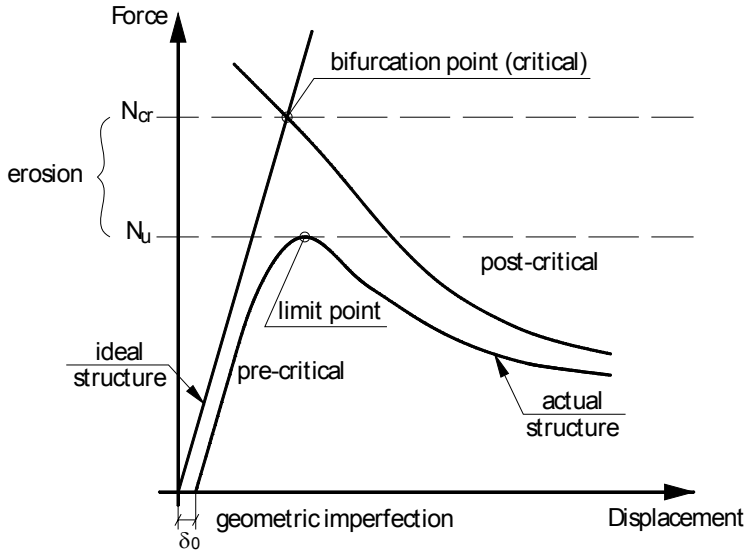

Fig. 1 – Critical and post-critical behaviour.

For a real structure, affected by a generic imperfection, δ_0, the bifurcation point does not appear anymore and, instead, the equilibrium *limit point* is the one characterizing the ultimate capacity, N_u, of the structure. The difference between N_{cr} and N_u represents the *Erosion of the Critical Bifurcation Load* (*ECBL*), due to the imperfections. The model in Fig. 1 can also be applied in case of structures which might be prone to subsequent buckling modes interacting in the bifurcation point, i.e.: a primary mode which, if it does not cause the failure of the structure, play the role in the pre-critical path (e.g. local buckling in case of slender

thin-walled members), and the secondary mode which, at the end, that is the one causing the failure (this will be the post-critical mode). Roughly, this is the description of *instability mode interaction*.

The meaning of the *mode interaction* refers to the *erosion* of critical bifurcation load in case of interaction of two (or more) buckling modes associated with the same, or nearly the same, critical load; it happens when the mode simultaneity is due to the results of design and/or imperfections. A well-known example of *mode interaction* is the coupling of local or distortional buckling with the overall buckling in the case of thin-walled cold-formed steel members, or the coupling between local buckling of class 4 web with the lateral-torsional buckling of plated beam.

In almost all practical cases, the mode interaction, obtained by coupling of a local instability with an overall one, is a result of design (e.g. calibration of mechanical and geometrical properties of a member) and has a nonlinear nature:

- Coupling by design occurs when the geometric dimensions of structure are chosen such as two or more buckling modes are simultaneously possible. For this case, the optimization based on the simultaneous mode design principle plays a very important role and the attitude of the designer towards this principle is decisive. This type of coupling is the most interesting in practice because, even the erosion of critical buckling load is maximum in the interactive range, the ultimate buckling strength still remains maximum in this range;
- Nonlinearity characterizes the post-buckling behaviour of coupling of instability modes and is due to design and the presence of the geometrical imperfections which is indispensable for coupling; this coupling doesn't exist for ideal structure. For instance, this is the case of the interaction between flexural buckling and flexural-torsional buckling of some mono-symmetrical cross-section.

Figure 2 illustrates such a case for a mono-symmetrical T-section in compression, studied in Timisoara [12], which is prone to the mode interaction between flexural and flexural-torsional modes. Due to the imperfections the erosion of critical bifurcation load occurs. The erosion is maximum in the coupling point vicinity (Fig. 1). For bar members, an interactive slenderness range, in which sensitivity to imperfections is increased, may be identified. Depending on imperfection sensitivity, classes of interaction types, characterized by specific levels of erosion intensity, may be defined.

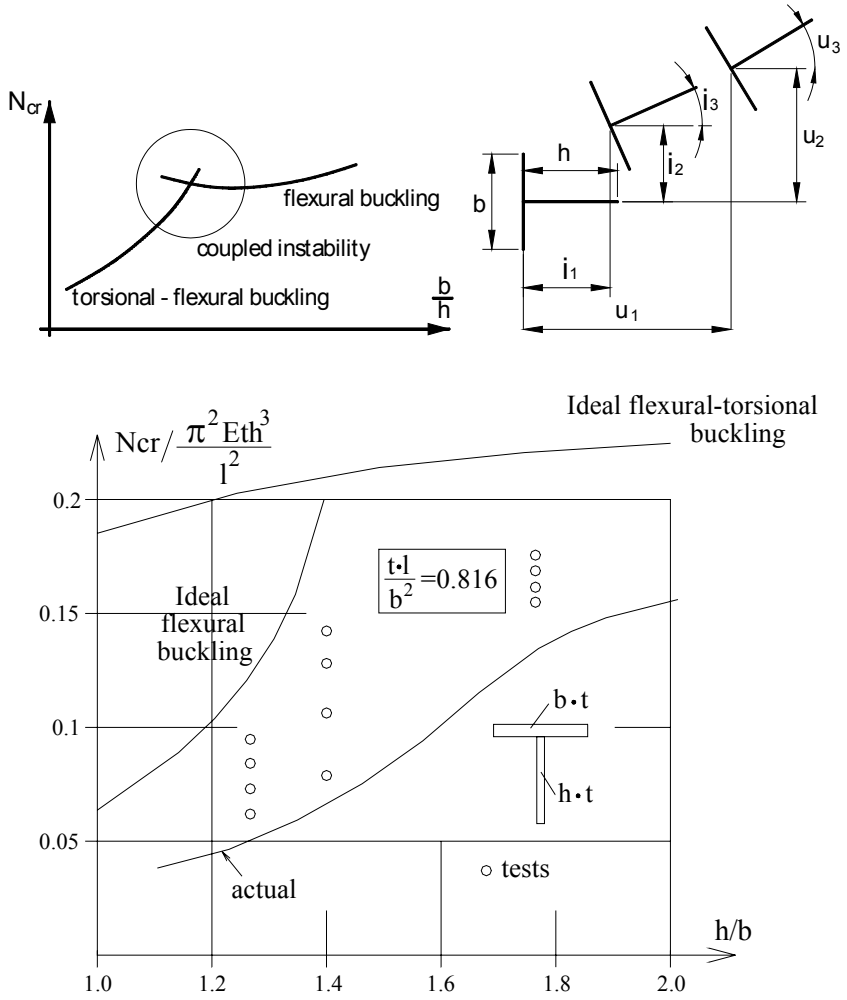

Fig. 2 – Coupled instability by design: example for T-section [12].

Given a member in compression and assuming *two simultaneous buckling modes* which might couple (Fig. 3), the perfect member fails under interactive critical buckling load, N_{cr}, while the real capacity of the actual member will be the ultimate load, N_u. The erosion, ψ, can be expressed as follows:

$$\psi = 1 - \overline{N}_u / \overline{N}_{cr}, \tag{1}$$

and

$$\overline{N}_u = (1 - \psi)\overline{N}_{cr}. \tag{2}$$

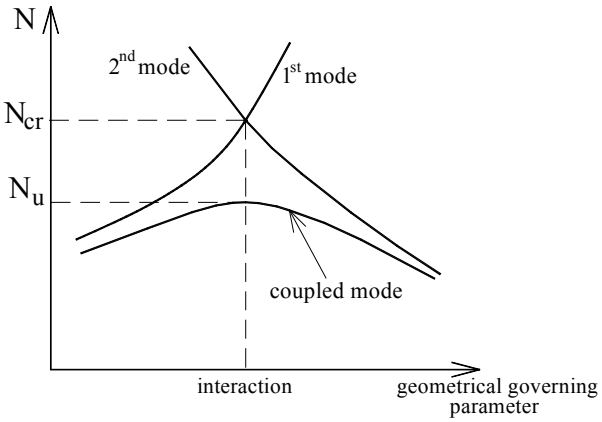

Fig. 3 – Generic model of two mode interaction.

An *erosion factor* ψ can be defined and used as a *measure* of erosion of Theoretical critical load. Gioncu [13] has ranked in four classes the mode interaction types in terms of erosion factor, as follows:

- class I: weak interaction (WI), $\psi \leq 0.1$;
- class II: moderate interaction (MI), $0.1 < \psi \leq 0.3$;
- class III: strong interaction (SI), $0.3 < \psi \leq 0.5$;
- class IV: very strong interaction (VI), $\psi > 0.5$.

Obviously, an appropriate framing of each mode interaction into a relevant class is very important because the methods of analysis used for design have to be different from one class to another. Week or moderate interactions could be controlled by code-based design procedures, the partial safety coefficients being able to keep safe those structures; higher interaction classes, particularly SI and VI, need for more refined examination, in principle using advance numerical methods and taking into account for relevant imperfection scenarios.

Interaction classes can be associated with erosion levels (Fig. 4).

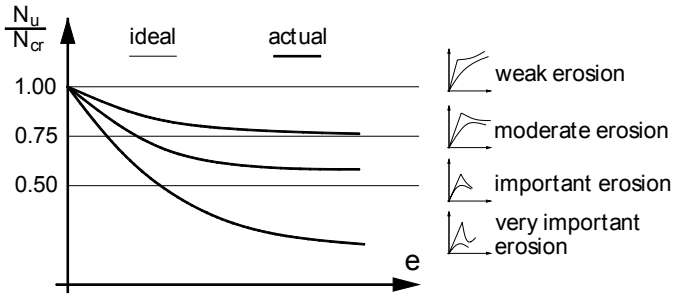

Fig. 4 – Erosion levels [13].

In case of thin-walled members, two types of interaction might occur. The first one is due to multiple local modes, which leads to a so called *localized* mode, and gives rise to an unstable post-critical behaviour. The second interaction, between the localized buckling mode and the overall buckling one, yields to a very unstable post-critical behaviour, with great erosion due to the imperfections. The multiple local buckling modes' interaction might generate a *localized* mode which subsequently can interact with an *overall mode*, with very destabilizing effects (Fig. 9, further on). Strong and very strong interactions are the result of this type of coupled instability. In such a case, very special design methods must be developed. Currently, such a phenomenon is characteristic for thin-walled columns in compression. Table 1 qualitatively indicates the erosion levels for mode interaction classes i.e.

Table 1
Coupled instabilities in bar members [14]

No.	Bar member type	Instability modes	Class of interaction
1.	Mono-symmetrical columns	F + FT = FFT	WI to MI $\psi \leq 0.3$
2.	Built-up columns	F + L = FL	MI $0.1 < \psi \leq 0.3$
3.	Thin-walled columns	F + L = FL FT + L = FTL (F + FT + L = FFTL)	SI to VI $\psi \geq 0.3$
		F + D = FD FT + D = FTD (F + FT + D = FFTD)	MI to SI $0.3 \leq \psi \leq 0.5$
4.	Thin-walled beams	LT + L = LTL LT + D = LTD	MI $\psi \leq 0.3$

Legend: F = flexural buckling ; FT = flexural-torsional buckling;
L = local buckling ; D = distortional buckling
WI = week interaction ; MI = moderate interaction ; SI = strong interaction;
VI = very strong interaction.

2. THEORETICAL BACKGROUND

2.1. SELECTIVE REVIEW

A number of important problems of structural stability are characterized by multiple buckling modes associated with the same critical buckling load [15]. Such problems are used to be known as *instability mode interaction*. The theoretical approach of this phenomenon, also addressed as *interactive* or *coupled buckling* involves the general asymptotic theory of instability. The background of structural theory and post-buckling behaviour of structures is given in books and state-of-art

articles by: Hutchinson & Koiter [16], Thompson & Hunt [17, 18], Budiansky [19], Koiter [20], and Flores & Godoy [21]. The books on bifurcation theory by Chow & Hale [22], Golubitsky & Schaeffer [23] and Gioncu & Ivan [24] related to the theory of critical and post-critical behaviour of elastic structures have to be considered as basic lectures for the readers interested on this topic.

When speaking about the *mode interaction*, implicitly refers to the *erosion* of theoretical critical bifurcation load in case of interaction of two (or more) buckling modes associated with the same, or nearly the same, critical load; it happens when the mode simultaneity is due to the results of design and/or imperfections [25]. A well-known example of such a mode interaction is the one resulting from the coupling of local or distortional buckling with overall buckling in case of a thin-walled cold-formed members. In such cases, the critical values corresponding to *global buckling mode* are significantly lower than *local buckling modes*, and their interaction can be considered within the first non-linear approximation [26].

A comprehensive approach of the problem of elastic interaction between local and global buckling modes is due to van der Neut [27], who provided the evidence that the sensitivity to imperfections of thin-walled columns in compression is maximum into the interactive buckling range, where critical buckling loads corresponding to local and global modes are closed to each other.

Koiter & Kuiken [28], two years after van der Neut, developed the method known as *method of slowly varying local mode amplitude*. In 1976 Koiter has published his *General Theory of Mode Interaction in Stiffened Plates and Shell Structures* [29], followed by the well-known book of Thompson & Hunt, *A General Theory of Elastic Stability* [17], in which the theory of interaction between coincident instability buckling modes is presented. On the same line, fundamental contributions to the problem of local-overall mode interaction of thin-walled sections are the studies of Thompson & Lewis [30]. Tvergaard [31,32] presented a method enabling to evaluate the erosion of ultimate capacity of interaction of overall mode, in post-buckling range, with plate local buckling mode, which is stable in post-buckling range, as it was the case of van der Neut problem.

Based on van der Neut principle and applying the Ayrton-Perry equation [33], Dubina [14] proposed the *Erosion of Critical Bifurcation Load* (ECBL) approach, enabling to evaluate the theoretical erosion of critical load into the interactive buckling range. Later, based on the real behaviour of thin-walled stub columns and short beams, Ungureanu & Dubina [34,35] used in the interactive local-overall buckling analysis the sectional plastic mechanism strength instead of traditional *effective section* and, the ECBL approach, in order to express the plastic-elastic interactive buckling of thin-walled cold-formed steel members.

In the last two decades intensive progress in studying the mode interaction problems was achieved due to the development of specific numerical methods. Since the late 1980s, the Generalized Beam Theory (GBT) [36, 37, 38, 39, 40, 41]

has been developed extensively. Particularly connected to the present topic, Camotim & Dinis [42] performed extended numerical studies, using FEM and GBT, to study the elastic post-buckling behaviour of cold-formed steel columns affected by mode interaction phenomena involving distortional buckling, namely local/distortional, distortional/global (flexural-torsional), local/distortional/global mode interaction and also sensitivity to imperfections of thin-walled cold-formed steel members.

Alternatively, another approach has been proposed based on conventional FSM, i.e. CUFSM [43], freely available at the www.ce.jhu.edu/bschafer/cufsm. The recently developed constrained Finite Strip Method (cFSM) provides a means to simplify thin-walled member stability solutions through its ability to identify and decompose mechanically meaningful stability behaviour, notably the formal separation of local, distortional, and global deformation modes. In this version the solution has been expanded to allow for general end boundary conditions [44].

Another design method, which can be framed in the class of semi-analytical methods, is *Direct Strength Method* [45], which practically replaces the *effective width* concept with the *effective stress* one. The method explicitly incorporates local or distortional and Euler buckling and does not require calculations of the effective properties. The procedure is an alternative to *effective width* method. Direct Strength Method has been adopted in 2004 as design method in Appendix 1 to the *North American Specification for the Design of Cold-Formed Steel Structural Members* [46].

In the last years, very interesting developments based on the fundamental theoretical works of Koiter [25] have been developed by Garcea et al. [47, 48]. The asymptotic approach, derived as a finite element implementation of Koiter's nonlinear theory of elastic stability, could be a convenient alternative by providing an effective and reliable strategy for predicting the initial post-critical behaviour in both cases of limit or bifurcation points. Its main advantage lies in the possibility of performing an efficient and reliable imperfection sensitivity analysis, even in cases of multiple, nearly coincident, buckling loads.

2.2. THE VAN DER NEUT MODEL

As already mentioned, a milestone achievement enabling for both understanding and practical characterisation of the local-global mode interaction problem is the pioneering study conducted by van der Neut [27], which has clearly demonstrated the erosion of theoretical critical coupling due to imperfections.

In this case, the interaction occurred between the local buckling of the flanges and flexural buckling of a square box section column; only the flanges have been considered to be active, while the web role was to connect them. Fig. 5a shows the buckling curve of the van der Neut column without local or overall imperfections. For lengths greater than L_1 the column fails in overall Euler buckling, i.e.

$$N_E = \pi^2 EI / L^2 . \tag{3}$$

For shorter lengths, the local buckling load, i.e.

$$N_{cr,L} = 2\frac{k_\sigma \pi^2 E}{12(1-\nu^2)}\left(\frac{t}{d}\right)^2 \tag{4}$$

is reached before Euler buckling takes place (t is the thickness and d is the width of flanges, ν is the Poisson's ratio and $k_\sigma = 4$, the plate buckling coefficient). In the locally buckled shape, a reduced bending stiffness of the column, given by ηEI, is considered, where η is the slope of the load-strain diagram of the flange plate in the post-local buckling range. van der Neut has considered the results of work by Hemp [49], who demonstrated that η is fairly constant over an extended strain range past the local buckling point and can be taken as $\eta = 0.4083$ for plates of which the longitudinal edges are free to pull in. As a result, the reduced overall buckling load in the post-local buckling range is given by $N_u = \eta N_E$, with $N_E = \pi^2 EI / L^2$. For column lengths between L_1 and L_2, the equilibrium at a load N_L is stable if:

$$\frac{2\eta}{1+\eta}\pi^2 \frac{EI}{L^2} > N_L . \tag{5}$$

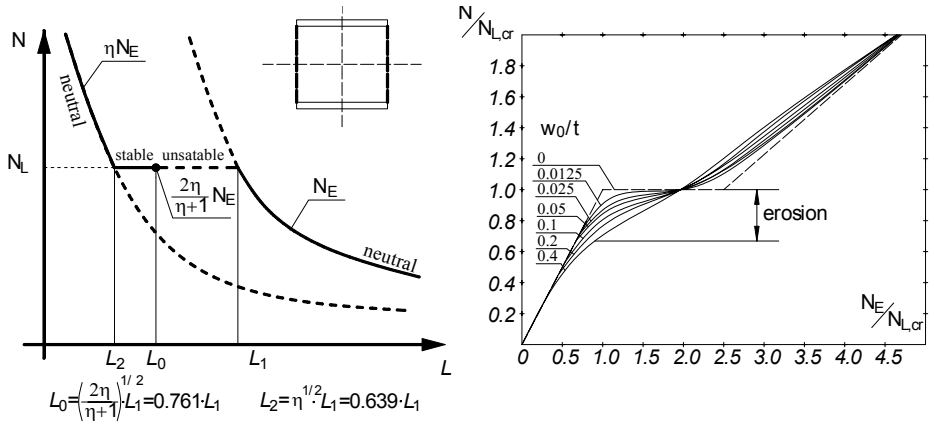

Fig. 5 – a) The van der Neut curve [27]; b) effect of a local imperfection on the buckling load [27].

Eqn. (5) expresses that the column post-buckling capacity, given by Engesser's double modulus formula, has to be greater than the local buckling load N_L, and results in: $L_2 < L < L_0$, with $L_0 = 0.761 L_1$. Columns with $L_0 < L < L_1$ are in a state of unstable equilibrium once the local buckling load is reached and collapse explosively (e.g. snap through effect).

In a second step, van der Neut considered a local imperfection affine with the local buckling mode. In this case, η was obtained from a Ritz-Galerkin approximate solution of the von Karman equations. Fig. 5b displays the non-dimensional

buckling load $N/N_{L,cr}$ function of $N_E/N_{L,cr}$ for different values of w_0/t, where w_0 is the local imperfection amplitude and t, is the flange thickness. It is seen that the local imperfection can cause a severe reduction in column capacity, and that the effect is most pronounced in the vicinity of the point where $N_E = N_{L,cr}$. For instance, a reduction (e.g. erosion) of 30% was calculated for $w_0/t = 0.2$. It was also demonstrated that, in the region where the perfect column displays unstable collapse, the peak of the load-bar shortening curve gets smoothened out as a result of the imperfection and the instability almost vanishes for $w_0/t = 0.2$. Van der Neut [50] also investigated the effect of overall imperfections on the idealised column. The research concluded that the presence of an overall imperfection (e.g. bar deflection) has a similar negative effect on the column strength.

At the end, the most important observation of this study is the reduction of N, due to the initial imperfection of flanges which is most significant when $N_E = N_{L,cr}$. The ECBL approach, proposed by Dubina [14], presented on the following is based on that conclusion.

2.3. EROSION OF CRITICAL BIFURCATION LOAD – ECBL

To understand better mode interaction problem, let consider the theoretical elastic buckling modes (bifurcation) characterizing the instability of a thin-walled member in compression. The local mode could be local buckling (L) or distortional buckling (D), the lower of $N_{L,cr}$ or $N_{D,cr}$ being considered. Similarly, the overall mode might be either flexural (F) or flexural-torsional (FT). In Fig. 6, (L) and (F) modes are assumed in order to identify and qualify the erosion of (L) – (F) interaction. These modes are interacting into the *theoretical* coupling point (C_{th}), while the lowest value $N = N_{L,cr}$ with (F) into the *practical* coupling point (C_{pr}), allowing the theoretical, ψ_{th}, and practical, ψ_{pr}, erosions to be evaluated. In case, distinction can be made between local buckling strength $N_{L,cr}$ or $N_{D,cr}$ and ultimate stub column strength, $N_{L,u}$ or $N_{D,u}$, respectively. The $N_{L,u}$ and $N_{D,u}$ values are obtained considering the relevant imperfections, while for $N_{L,cr}$ and $N_{D,cr}$ there are no imperfections taken into account.

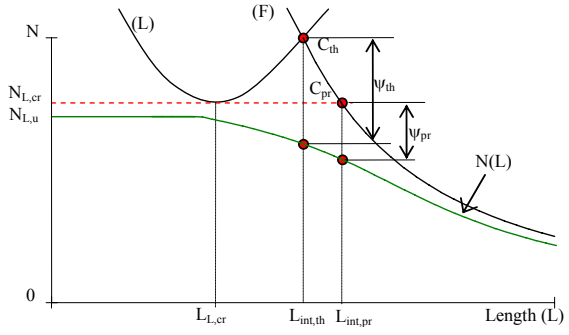

Fig. 6 – Theoretical and practical interaction of two buckling modes: distortional (L) and flexural (F).

To introduce the ECBL approach, firstly, the interpretation in terms of erosion of equation of European buckling curves, expressed in Ayrton-Perry format has to be done. The Ayrton-Perry equation, for the case of a member in compression, which is not prone to local buckling, but can undergoes buckling in post-elastic range, can be written in the form:

$$(1-\overline{N})(1-\overline{N}\overline{\lambda}^{-2}) = \alpha\overline{N}(\overline{\lambda}-0.2)\,, \tag{6}$$

where $\overline{\lambda}$ is the non-dimensional slenderness (flexural, $\overline{\lambda}_F$, or flexural-torsional, $\overline{\lambda}_{FT}$). It is easy to show the relation between the imperfection factor, α, and erosion coefficient, ψ [14]. In this case, the erosion of theoretical ultimate capacity in compression is due to the effect of imperfections and plastic deformations. The negative sign solution of Eqn. (6), in the point $\overline{\lambda}=1$ has to be taken equal with $(1-\psi)$, because it corresponds to the maximum erosion of theoretical critical load when no local buckling occurs, as shown by Eqn. (7), i.e.

$$\overline{N}(\overline{\lambda}=1,\alpha) = \frac{1}{2}\left[2+0.8\alpha-\sqrt{(2+0.8\alpha)^2-4}\right] = 1-\psi\,, \tag{7}$$

that gives

$$\alpha = \frac{\psi^2}{0.8(1-\psi)} \tag{8}$$

or

$$\psi = 0.4\left(\sqrt{5\alpha+\alpha^2}-\alpha\right). \tag{9}$$

In this case the erosion can be associated to the plastic-elastic interaction between the rigid plastic mode (plastic strength) of stub column ($\overline{\lambda}\le 0.2$) and the overall elastic buckling mode of the bar given by Euler formula, as shown in Fig. 7.

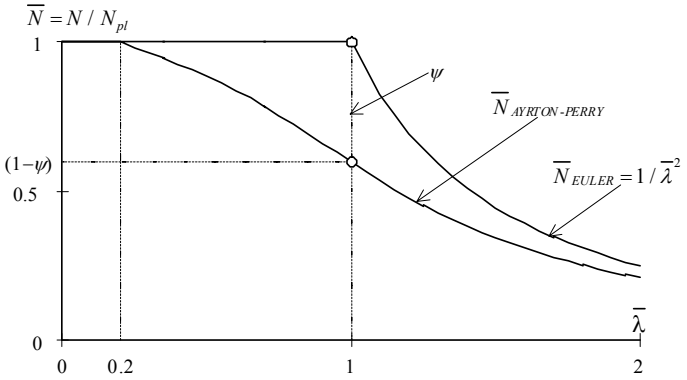

Fig. 7 – The erosion of bar buckling curve.

For local-overall mode interaction, the two theoretical simple instability modes assumed to interact in a thin-walled compression member are: (1) the Euler bar instability mode, $\overline{N}_E = N_E / N_{pl}$, $\overline{N}_E = 1/\overline{\lambda}^2$, and (2) the local instability mode, $\overline{N}_L = N_L / N_{pl}$ (Fig. 8).

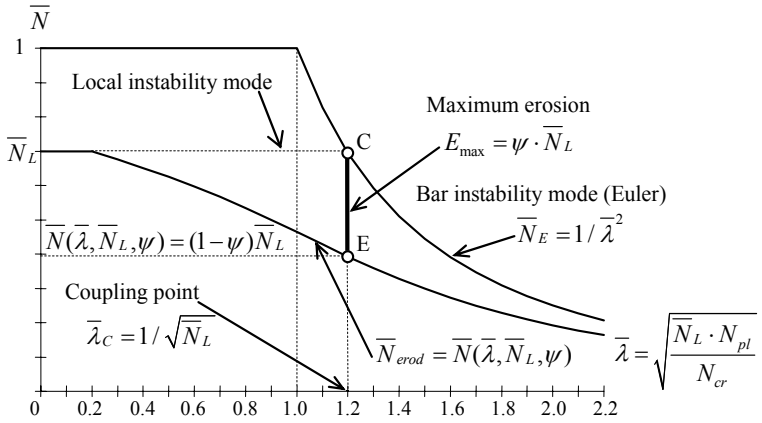

Fig. 8 – Definition of erosion in local-overall mode interaction via ECBL approach.

In this case, the maximum erosion of critical load, due to both, imperfections and coupling effect occurs in the coupling point, C ($\overline{\lambda}_C = 1/\sqrt{\overline{N}_L}$), where:

- $\overline{N} = N / N_{pl}$, $N_{pl} = A \cdot f_y$, where A is the area of the member cross-section and f_y is the yielding strength;
- $\overline{N}_L = N_L / N_{pl}$, where N_L is either local buckling mode or distortional buckling mode;
- $\overline{N}_E = N_E / N_{pl}$, the Euler critical buckling load.

The interactive buckling load, $\overline{N}(\overline{\lambda}, \overline{N}_L, \psi)$, pass through this point where the corresponding value of ultimate buckling load is $\overline{N}(\overline{\lambda}_C) = (1-\psi)\overline{N}_L$. It must be underlined that $\overline{N}_L$ does not rigorously represents the theoretical local buckling, but it is assumed to be the *lower bound* of that, and can be used as reference for strength of the cross-section corresponding to the local or distortional buckling mode. It enables to estimate the strength of the stub column and to obtain the coupling point C. On the other hand, the occurrence of local or distortional buckling, the stiffness of the member decreases significantly, resulting in a *jump of equilibrium* onto the overall buckling path. In this case, if compares Fig. 8 with Fig. 7, the effect of mode interaction is added to those of plastic deformations and imperfections, and the reference load for evaluation of erosion is not anymore $\overline{N} = N / N_{pl} = 1$, but $N_L / N_{pl} < 1$.

When local buckling occurs prior to bar buckling (as it was in the case of van der Neut problem), then the corresponding solution of Eqn. (10), i.e.:

$$(\overline{N}_L - \overline{N})(1-\overline{\lambda}^2\overline{N}) = \alpha(\overline{\lambda}-0.2)\overline{N} \tag{10}$$

in the coupling point *C* of Fig. 8 is:

$$\overline{N} = \frac{1+\alpha(\overline{\lambda}-0.2)+\overline{N}_L\overline{\lambda}^2}{2\overline{\lambda}^2} - \frac{1}{2\overline{\lambda}^2}\sqrt{\left[1+\alpha(\overline{\lambda}-0.2)+\overline{N}_L\overline{\lambda}^2\right]^2 - 4\overline{N}_L\overline{\lambda}^2} = \\ = (1-\psi)\overline{N}_L \tag{11}$$

which leads to

$$\alpha = \frac{\psi^2}{1-\psi}\frac{\sqrt{\overline{N}_L}}{1-0.2\sqrt{\overline{N}_L}}. \tag{12}$$

This represents the formula of α imperfection factor which should be introduced in European buckling curves in order to adapt these curves to local – overall buckling. Of course, following this approach, the definition of stub column (i.e. the lower value in the buckling curve) has to be adapted correspondingly.

When speaking about the erosion of theoretical buckling curve in the coupling point, distinction should be made between the erosion, ψ, which refers to the effect of both imperfections and coupling, and the reduced ultimate strength of member, characterized by the normalized local buckling strength, $\overline{N}_L$. This approach applies similarly for both local (L) and distortional (D) buckling modes, providing they are not interacting each other; the basic Ayrton-Perry formula, presented by Eqn. (6) does not change.

In case of a thin-walled steel member prone to local buckling, $\overline{N}_L = \overline{N}_{L,cr}$ can be approximated by $Q = A_{eff}/A$, where A is the area of gross cross-section, while A_{eff} is the effective area calculated using *effective width* method. In case of distortional buckling, $\overline{N}_L = \overline{N}_{D,cr} = N_{D,cr}/Af_y$, where $N_{D,cr}$ is the critical value of distortional buckling.

In order to evaluate the ψ erosion factor, two different methods are possible to this purpose i.e.: experimental and numerical method, respectively [14].

a) Experimental method. The experimental calibration method requires a relevant set of experimental values located in a close neighbourhood of the coupling point, called *coupling range*. Most often available experimental results scatter, as a result of unavoidable mechanical and geometrical imperfections. Consequently, the concerned specimens do not meet the main requirement of ECBL approach to have reduced member slenderness identical to the one locating

the coupling point ($\bar{\lambda}_C = 1/\sqrt{\bar{N}_L}$, see Fig. 8). Even in case of own dimensioned specimens, sized to be *theoretically* located in the coupling point, the imperfections produce an unavoidable scatter of the experimental results and require the work with a coupling range as well.

The selection of the relevant set of specimens should be performed by choosing among *existing results experimental samples reasonably close to the instabilities coupling point* (in terms of reduced slenderness). This is leading to the idea of using a *coupling range*, defined in terms of reduced slenderness as a vicinity of the coupling point, instead of working strictly in this point. A correct definition of coupling range limits is therefore of paramount importance for the selection of a relevant set of specimens. Extensive parametric studies [51] have indicated as acceptable an unsymmetrical coupling range defined around $\bar{\lambda}_c$ with left limit $\bar{\lambda}_1 = 0.85 \cdot \bar{\lambda}_c$ and the right limit $\bar{\lambda}_2 = 1.075 \cdot \bar{\lambda}_c$. All specimens with a reduced slenderness comprised between these two limits should be considered as reasonably close to the coupling point and selected as relevant experimental set.

b) Numerical method. Based on an advanced nonlinear inelastic FEM analysis and taking into account for the imperfections and cold-forming effect, the numerical models have to simulate relevant experimental values into the coupling range. However, the numerical method requires also some experimental results in order to calibrate the FEM model.

The previous approach can be very easily extended to the case of interactive local/lateral-torsional buckling of thin-walled beams [52]. Following the same procedure, the α_{LT} imperfection factor can be determined, i.e.:

$$\alpha_{LT} = \frac{\psi_{LT}^2}{1-\psi_{LT}} \cdot \frac{\sqrt{Q_{LT}}}{1-0.4\sqrt{Q_{LT}}}. \tag{13}$$

The new ECBL interactive approach for lateral-torsional buckling of thin-walled beams is similar to that of EN 1993-1-1, but instead of ϕ_{LT} given in EN 1993-1.1 the following value should be used:

$$\phi_{LT} = 0.5[1 + \alpha_{LT}(\bar{\lambda}_{LT} - 0.4) + \bar{\lambda}_{LT}^2], \tag{14}$$

with α_{LT} calculated from Eqn. (13) in terms of the erosion factor ψ_{LT}.

Finally, it appears easier to evaluate experimentally and/or numerically the erosion coefficients, ψ, for specific types of cold-formed steel sections and, on this basis, to calibrate relevant α imperfection factors, in order to be implemented in the EN 1993-1-1. Examples of calibration of α imperfection factors are presented in [14, 34, 35, 52–57].

3. EXAMPLES OF α IMPERFECTION FACTORS CALIBRATION

3.1. PLASTIC-ELASTIC INTERACTIVE BUCKLING VIA ECBL APPROACH [34,35]

Cold-formed steel sections are traditionally considered with no plastic capacity, and consequently non-ductile, mainly due to wall slenderness involving local instability phenomena. However, even they do not have sufficient plastic rotation capacity to form plastic hinges, they can form local plastic mechanisms.

In case of a thin-walled member multiple local buckling modes may occur simultaneously under the same critical load. For a long member, multiple local buckling modes, e.g. *m-1*, *m*, *m+1*, characterized by L_{m-1}, L_m and L_{m+1} half wave-lengths, respectively may interact each other and give rise to an unstable post-critical behaviour called *localization of the buckling pattern* (Fig. 9).

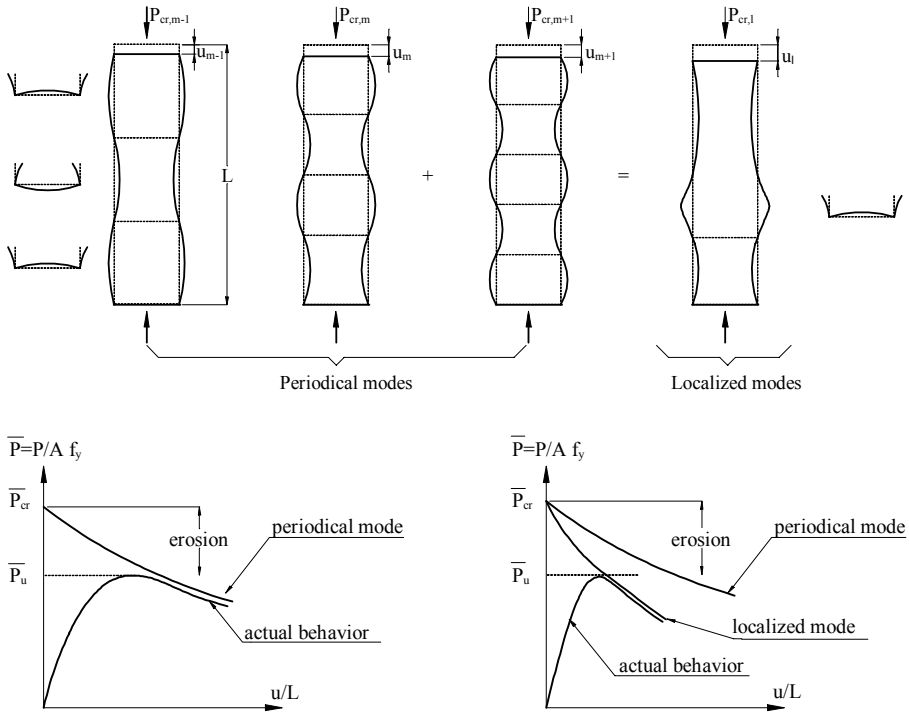

Fig. 9 – Periodical local modes and localization of buckling patterns in case of flanges of a plain channel section in compression.

The localized buckling mode is in fact an interactive or coupled mode. This is a *first* interaction, which may occur prior the overall buckling mode of the member. The *second* interaction, between the localized buckling mode and the overall one is really dangerous because it is accompanied by a very strong erosion of critical

bifurcation load. When localization of buckling patterns occurs, the member post-buckling behaviour is characterized by large local displacements, in the inelastic range, which produce the plastic folding of walls, and the member, falls into a plastic mechanism [58].

Starting from this real behaviour of thin-walled stub columns and short beams, Ungureanu & Dubina [34, 35] used the ECBL approach in order to express the plastic-elastic interactive buckling of thin-walled members. The main problem of this approach is to evaluate properly the plastic strength of thin-walled members, via the local plastic mechanism theory and after, the erosion of critical load into the *plastic-elastic coupling range*.

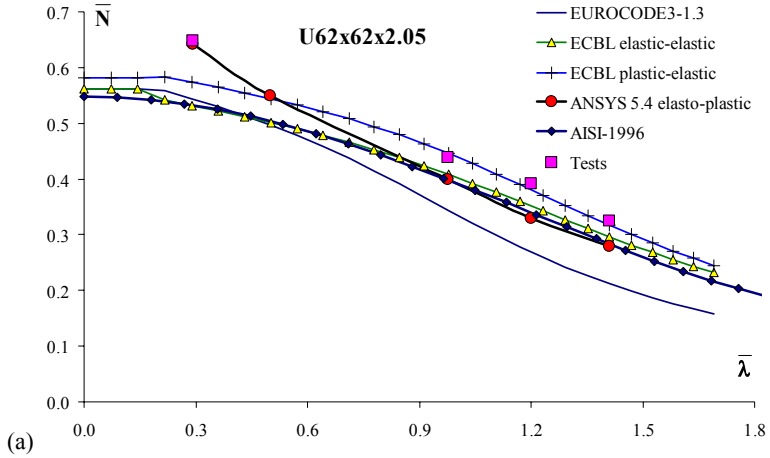

(a)

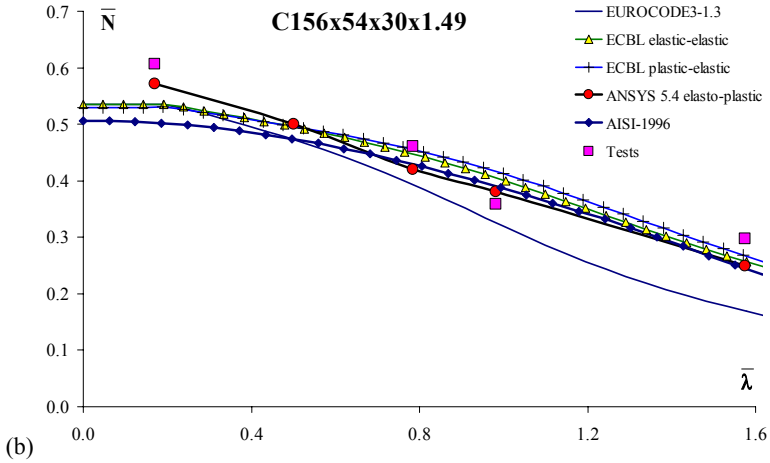

(b)

Fig. 10 – Numerical/Experimental comparison for compression members [34].

Following exactly the same way as for the elastic local-overall interactive buckling, it results the α imperfection factor for the plastic-elastic interactive buckling:

$$\alpha = \frac{\psi^2}{1-\psi} \cdot \frac{\sqrt{Q_{pl}}}{1-0.2\sqrt{Q_{pl}}}, \tag{15}$$

where

$$Q_{pl} = \overline{N}_{pl,L} = \frac{N_{pl,m}}{A \cdot f_y} \tag{16}$$

and $N_{pl,m}$ is the local plastic mechanism strength.

In case of members in compression, Fig. 10 presents the $ECBL_{pl\text{-}el}$ results, compared with those from FEM elastic-plastic analysis, the ECBL elastic-elastic, $ECBL_{el\text{-}el}$, and experimental tests [34]. It is easy to observe the quality of $ECBL_{pl\text{-}el}$ results are excellent, particularly in the interactive zone, e.g. $0.4<\overline{\lambda}<1.6$.

In case of slender beams, experimental data were used to compare the $ECBL_{pl\text{-}el}$ and $ECBL_{el\text{-}el}$ results with those of EN1993-1-3 and AISI-1996 results. Figure 11 shows again that $ECBL_{pl\text{-}el}$ model confirm its accuracy [35].

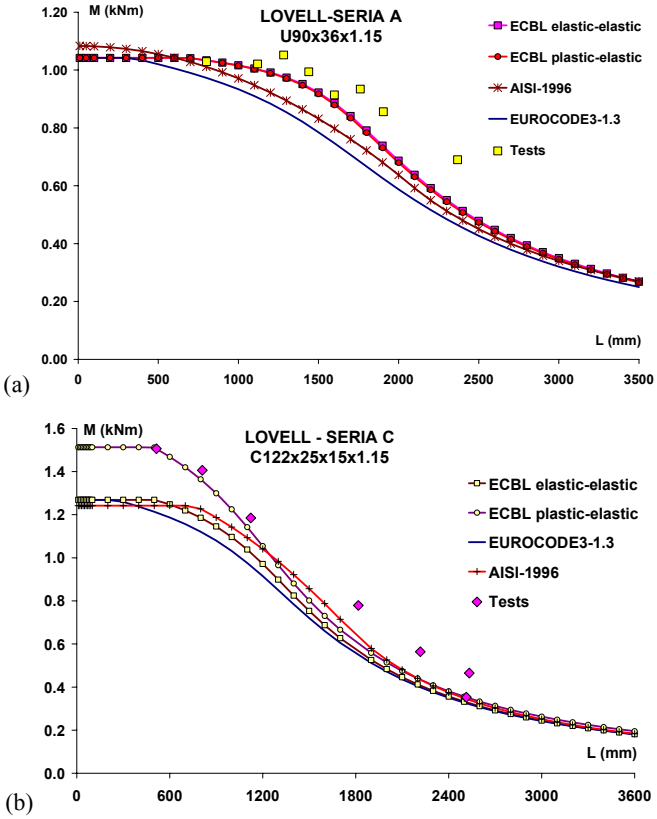

Fig. 11 – Numerical/Experimental comparison for bending members [35].

The local rigid-plastic model, describes properly the behaviour of thin-walled short members. This model is consistent with the real phenomenon of stub columns and short beams failure and is confirmed by test results and advanced elastic-plastic FEM analysis. The plastic-elastic interactive model naturally describes the phenomenon of the interactive buckling of thin-walled members. The *ECBL plastic-elastic interactive approach*, based on the erosion theory of coupled bifurcation, is much more rigorous and understandable than the semi-empirical methods used for the buckling curves in existing design codes.

3.2. EROSION OF BUCKLING STRENGTH DUE TO THE INFLUENCE OF THE SHAPE OF SECTIONAL GEOMETRICAL IMPERFECTIONS [53]

Based on numerical simulations and applying the ECBL approach, Dubina & Ungureanu [53] have systematically studied the influence of size and shape of sectional geometrical imperfections on the ultimate buckling strength of plain and lipped channel sections, both in compression and bending, in order to evaluate the erosion of theoretical strength when sectional and overall buckling modes interact. Fig. 12 explains the erosion phenomenon applied to this problem [14].

The following notations were used:

$\overline{N}=N/N_{pl}$, where N is the ultimate strength of the member; N_{pl} is corresponding full plastic strength;

$\overline{N}_{L,th}=N_{L,th}/N_{pl}$, with $N_{L,th}$ the ultimate theoretical stub column strength;

$\overline{N}_L=N_L/N_{pl}$, N_L being the ultimate strength of imperfect stub column;

$\overline{\lambda}=\sqrt{N_L/N_{cr}}$, the reduced slenderness of the member.

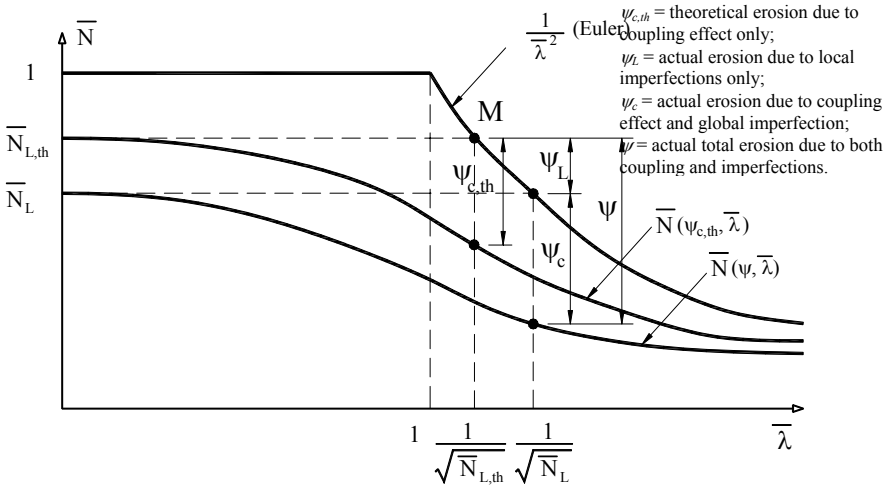

Fig. 12 – The interactive buckling model based on the ECBL theory [53].

Maximum erosion ψ of theoretical interactive buckling strength is calculated in regard with the theoretical interaction point, M ($\bar{\lambda}_{\text{int}} = 1/\sqrt{\overline{N}_{L,th}}$), and is:

$$\psi = \overline{N}_{L,th} - \overline{N}(\bar{\lambda} = 1/\sqrt{\overline{N}_L}) . \tag{16}$$

The total erosion can be associated with the α (α_{LT}) imperfection factor used in European buckling curves for members in compression (bending), by means of ECBL formula:

Compression Bending

$$\alpha = \frac{\psi^2}{1-\psi} \cdot \frac{\sqrt{\overline{N}_L}}{1-0.2\sqrt{\overline{N}_L}} \qquad \alpha_{LT} = \frac{\psi_{LT}^2}{1-\psi_{LT}} \cdot \frac{\sqrt{\overline{M}_L}}{1-0.4\sqrt{\overline{M}_L}} . \tag{17}$$

The $\overline{N}$ and $\overline{M}$ values can be computed for perfect and imperfect shapes of both, cross-section and member. Therefore, the erosion can be evaluated for different imperfection cases. If no imperfections, the evidence of interactive buckling effect only will be observed. Further, the values of α (α_{LT}) imperfection sensitivity factor used in European buckling curves have been evaluated for all these imperfection shapes. Tables 2 and 3 show the main results of this study [53].

Table 2

α imperfection sensitivity factor for members in compression [53]

Plain channel 96×36×1.5					Lipped channel 96×36×12×1.5				
Shape of imperf.	Imperfection mode	ψ	α	Buck-ling curve	Shape of imperf.	Imperfection mode	ψ	α	Buck-ling curve
	- local buckling PL1 (symmetric sine shape)	0.450	0.322	b		- local buckling LL1 (symmetric sine shape)	0.286	0.109	a_o
	- local buckling PL2 (asymmetric sine shape)	0.442	0.304	b		- local buckling LL2 (asymmetric sine shape)	0.283	0.105	a_o
	- distortional buckling PD3 (symmetric sine shape)	0.466	0.354	c		- distortional buckling LD3 (symmetric sine shape)	0.492	0.461	c
	- distortional buckling PD4 (asymmetric sine shape)	0.471	0.365	c		- distortional buckling LD4 (asymmetric sine shape)	0.404	0.265	b

Table 3
α_{LT} imperfection sensitivity factor for members in bending [53]

Plain channel 96×36×1.5					Lipped channel 96×36×12×1.5				
Shape of imperf.	Imperfection mode	ψ_{LT}	α_{LT}	Buck-ling curve	Shape of imperf.	Imperfection mode	ψ_{LT}	α_{LT}	Buck-ling curve
	- distortional buckling PD2 (the imperf. is constant over the length)	0.311	0.140	a		- distortional buckling LD1 (the imperf. is constant over the length)	0.355	0.292	b
	- distortional buckling PD7 (asymmetric sine shape)	0.312	0.142	a		- distortional buckling LD4 (asymmetric sine shape)	0.411	0.422	c

The appropriate identification and selection of imperfection shape and size associated to the relevant instability mode is crucial for ultimate strength analysis. In a two-mode interacting buckling (e.g. local-overall interaction) different shapes of local-sectional imperfections have different effects on the ultimate strength of the member. The values of α imperfection factor prove the higher sensitivity of distortional-overall interactive buckling to sectional imperfections. This fact can be explained by the lower post-critical strength reserve of distortional mode if coupled with local one.

3.3. DISTORTIONAL-OVERALL MODE INTERACTION OF PERFORATED PALLET RACK UPRIGHTS. IMPERFECTION SENSITIVITY ANALYSIS

The sections currently used in pallet rack uprights are particularly prone to distortional-overall interaction. An extensive experimental study on pallet rack uprights in compression has been carried out at the Politehnica University of Timisoara on the aim to observe the erosion of theoretical buckling load due to both coupling effect and imperfections for this type of interaction. The experimental program was extensively presented in [54].

Two cross-sections of the same typology but different sizes, RS125×3.2 and RS95×2.6, have been considered, of perforated-to-brut cross-section ratios (A_N/A_B) of 0.806 and 0.760, respectively. Their brut and perforated (i.e. net) sections are shown in Fig. 13 together with the perforations details. The pitch is 50mm for both studied sections.

Both perforated and unperforated section specimens have been tested, of calibrated lengths for: stub columns (s); upright member specimens for distortional buckling (u); specimens of lengths equal with the half-wave length for distortional buckling (d); specimens of lengths corresponding to interactive buckling range (c).

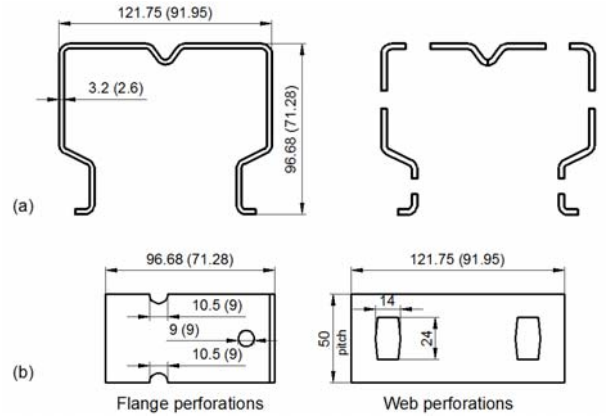

Fig. 13 – a) Brut and perforated specimen cross-section; b) perforation details [54].

Table 4 presents the failure modes for each type of the tested specimen/ section. The following notations have been used: S – Squash, DS – symmetrical distortional buckling, FT –flexural-torsional buckling, F – flexural buckling Additional experimental tests have been done in order to determine the mechanical properties of the material. A set of samples were tested from the base material. Additional series of tests on coupons cut over the cross-section of specimens without perforations was done for both types of sections to determine the increase of yield strength, ultimate tensile strength and residual stresses. In what concerns the geometric imperfections, all tested specimens were measured. Two types of imperfections were recorded, i.e. (a) sectional and (b) global.

Table 4
Failure modes for tested sections

Section / Test type	RS95×2.6 brut	RS95×2.6 perforated	RS125×3.2 brut	RS125×3.2 perforated
Stub (s)	S	S/DS	DS	DS
Distortional (d)	DS	DS	DS	DS
Upright (u)	F or FT	F or FT	DS	DS
Interactive buckling (c)	DS+F or DS+FT	DS+F or DS+FT	DS+F or DS+FT	DS+F or DS+FT

Advanced numerical models (i.e. GMNIA) have been applied to simulate the behaviour of studied sections, using the commercial FE program ABAQUS/CAE. The numerical models were calibrated to replicate the physical experimental tests. It must be underlined that for all considered numerical models, the failure modes were in accordance with the failure modes observed in experimental tests (see Fig. 14). The calibrated numerical models were validated against experimental tests for all tested sets of profiles. Table 5 presents the values of ultimate load from numerical simulations and the experimental ones for all types of members ((s), (u), (d), (c)), for both RS125×3.2 and RS95×2.6 cross-sections, with and without perforations. For details see [55, 56].

On the following the numerical investigations on the sensitivity to imperfections of pallet rack sections in compression, having the member length equal to the interactive buckling length, using ECBL approach are summarized [57, 59]. On this purpose, FE analyses were performed to simulate the influence of different types of imperfections in the coupling point. Because the interest is to observe the erosion of critical bifurcation load, this time, the ECBL approach is applied considering the distortional critical load, obtained for the relevant section by an eigen buckling analysis, in interaction with Euler buckling of the corresponding bar member

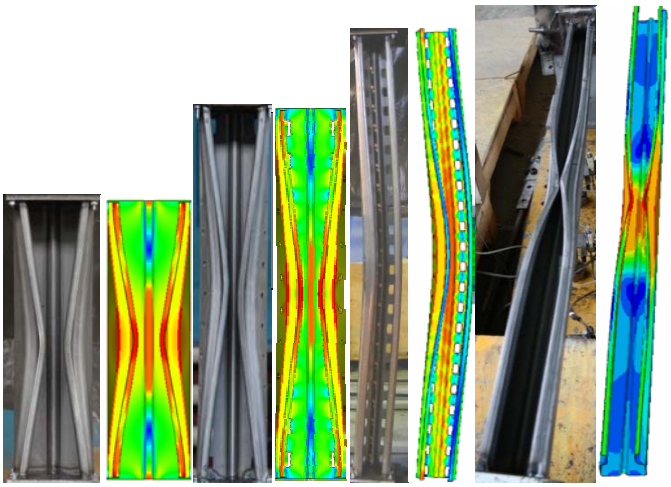

Fig. 14 – Failure modes: Experimental vs. FE models [55, 56].

Table 5
Ultimate load [kN]: experimental vs. FEM [55, 56]

RSBs125×3.2		RSNs125×3.2		RSBs95×2.6		RSNs95×2.6	
EXP	FEM	EXP	FEM	EXP	FEM	EXP	FEM
487.05	486.13	411.02	422.98	338.88	335.15	274.33	272.01
RSBd125×3.2		RSNd125×3.2		RSBd95×2.6		RSNd95×2.6	
EXP	FEM	EXP	FEM	EXP	FEM	EXP	FEM
440.79	440.78	394.62	397.04	325.10	331.05	262.67	255.47
RSBu125×3.2		RSNu125×3.2		RSBu95×2.6		RSNu95×2.6	
EXP	FEM	EXP	FEM	EXP	FEM	EXP	FEM
386.72	384.40	347.26	344.00	279.65	285.96	223.33	231.89
RSBc125×3.2		RSBc125×3.2		RSBc95×2.6		RSBc95×2.6	
EXP	FEM	EXP	FEM	EXP	FEM	EXP	FEM
317.89	316.67	293.62	292.9	220.29	220.26	168.88	177.11
(s) Stub columns; (d) Specimens of lengths equal with the half-wave length of distortional buckling; (u) Upright member specimens; (c) Specimens of lengths corresponding to interactive buckling range. N/B – perforated/brut							

Table 6 shows the reference values for critical and ultimate sectional loads obtained numerically and experimentally for the studied sections. Table 7 presents the lengths corresponding to the theoretical interactive buckling loads determined via the ECBL approach, in the interactive buckling point for each section [57, 59].

Table 6
Sectional capacity and distortional buckling load [57]

Section	RSN125×3.2	RSN95×2.6
Length [mm]	600	500
Distortional buckling load* ($N_{cr,D}$) [kN]	370.48	340.78
Distortional ultimate load** ($N_{D,u}$) [kN]	388.35	---
Stub ultimate load*** ($N_{S,u}$) [kN]	407.79	279.27
Squash load**** (N_{pl}) [kN]	480.94	286.72
* distortional buckling load determined using LBA; ** experimental failure load corresponding to "distortional" specimens – mean values; *** experimental failure load corresponding cu stub column specimens – mean values; **** $N_{pl}=A\cdot f_y$		

Table 7
Lengths corresponding to the theoretical interactive buckling [57]

Profile	$N_{cr,D}$ [kN]	N_{pl} [kN]	$\overline{N}_D$	Coupling length [mm]
RSN125	370.48	480.94	0.770	2559
RSN95	340.78	286.72	1.000	1667

It can be observed that for RS95N cross-sections, the critical load corresponding to distortional buckling is greater than the cross-section squash load. In this case the $\overline{N}_D$ value has to be limited to 1.00. Based on this limitation for RS95 section, with and without perforation, there is no classical interactive buckling, but we could speak about a local plastic – elastic global buckling interaction.

On the following, an imperfection sensitivity study was conducted in order to identify the most critical imperfection or combination of imperfections.

Fig. 15 shows the geometrical imperfections, considered in the analysis, i.e. distortional (d ±), flexural about the minor axis (f ±), and coupling of these two (f ± d ±). Also, load eccentricities, located on the axis of symmetry, were taken into consideration.

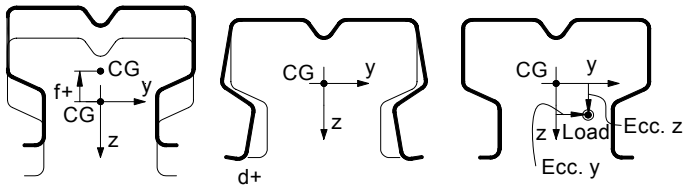

Fig. 15 – Example of considered simple imperfections (f and d) [57, 59].

In case of flexural-torsional buckling (FT), both initial deflection and initial twisting imperfection (ft) were considered together, according to Australian Standard AS4100 [60]. Due to the fact that the global flexural buckling mode about the minor axis has the minimum value for the studied sections the global imperfection considered for coupling was considered a global bow imperfection.

The imperfections used for this study were: distortional symmetric imperfection (ds), distortional asymmetric imperfection (da) (only for RSN125×3.2 section), flexural bow imperfection about the minor inertia axis (f), loading eccentricities on both axes (independent and coupled – EY, EZ, EY-EZ) and flexural-torsional imperfection (FT). The distortional imperfection, symmetric and asymmetric, was scaled to 0.5t, 1.0t and 1.5t, the flexural bow imperfection was scaled to L/750, L/1000 and L/1500, while the flexural-torsional imperfection was considered in accordance with the provisions of Australian design code [3.60]. The loading eccentricities were varied on both sectional axes, with ± 2 mm, ± 4 mm, ± 6 mm, independently (e.g. *EZ-4* means –4 mm eccentricity about z-axis) and together, as an oblique eccentricity (e.g. *EY-EZ4* means + 4 mm eccentricity about y-axis and +4 mm about z-axis).

Table 8 presents the considered simple imperfections, sectional, global and loading eccentricities for RSN125×3.2 section together with ψ erosion coefficient and α imperfection factors for simple imperfections.

In Table 8 can be easily observed that, for simple imperfections, symmetric distortion imperfection and major axis eccentricities give higher values for erosion coefficient than those corresponding to flexural and flexural-torsional imperfections.

Table 9 presents the coupled imperfections considered for the RSN125×3.2 section, i.e. f – L/750, ds – 0.5t; f – L/750, ds – 1.5t; f – L/1500, ds – 0.5t and f – L/1500, ds – 1.5t, combinations coupled with various types of eccentricities. It is easy to observe that the combination (f – L/750, ds – 1.5t) of imperfections is the most critical one. However, statistically is not recommended to combine all imperfections to cumulate their negative effects, because their random compensation.

Table 8
ψ erosion coefficients and α imperfection factors for simple imperfections

Imperfection	RSN125×3.2			Imperfection	RSN125×3.2	
	ψ	α			ψ	α
ds – 0.5 t	0.236	0.078		EZ -6	0.313	0.152
ds – 1.0 t	0.339	0.185		EZ -4	0.272	0.108
ds – 1.5 t	0.398	0.280		EZ -2	0.210	0.059
da – 0.5 t	0.152	0.029		EZ +2	0.216	0.063
da – 1.0 t	0.245	0.085		EZ +4	0.255	0.093
da – 1.5 t	0.321	0.162		EZ +6	0.285	0.121
f – L/750	0.240	0.081		EY-EZ 0	0.157	0.031
f – L/1000	0.216	0.063		EY-EZ +6	0.321	0.162
f – L/1500	0.181	0.043		EY-EZ +4	0.276	0.112
ft	0.240	0.081		EY-EZ +2	0.215	0.063
EY +2	0.169	0.037		EY-EZ -2	0.223	0.068
EY +4	0.196	0.051		EY-EZ -4	0.270	0.106
EY +6	0.224	0.069		EY-EZ -6	0.307	0.145

Table 9
ψ erosion coefficients and *α* imperfection factors for coupled imperfections

Imperfection	ψ	α	ψ	α	ψ	α	ψ	α
	f – *L*/750, ds – 0.5*t*		f – *L*/750, ds – 1.5*t*		f – *L*/1500, ds – 0.5*t*		f – *L*/1500, ds – 1.5*t*	
EY 2	0.339	0.185	0.440	0.368	0.302	0.139	0.422	0.328
EY 4	0.342	0.189	0.442	0.373	0.305	0.142	0.423	0.330
EY 6	0.346	0.195	0.443	0.375	0.310	0.148	0.425	0.334
EZ 6	0.425	0.334	0.493	0.510	0.411	0.305	0.483	0.480
EZ 4	0.404	0.292	0.479	0.469	0.384	0.255	0.467	0.436
EZ 2	0.376	0.241	0.461	0.420	0.350	0.201	0.447	0.385
EZ -2	0.279	0.115	0.413	0.309	0.174	0.039	0.387	0.260
EZ -4	0.194	0.050	0.374	0.238	0.228	0.072	0.326	0.168
EZ -6	0.240	0.081	0.276	0.112	0.264	0.101	0.261	0.098
EY-EZ 0	0.240	0.081	0.440	0.368	0.301	0.138	0.421	0.326
EY-EZ 6	0.430	0.345	0.495	0.517	0.414	0.311	0.485	0.486
EY-EZ 4	0.406	0.295	0.480	0.472	0.386	0.258	0.467	0.436
EY-EZ 2	0.377	0.243	0.462	0.422	0.351	0.202	0.447	0.385
EY-EZ -2	0.280	0.116	0.413	0.309	0.182	0.043	0.387	0.260
EY-EZ -4	0.218	0.065	0.376	0.241	0.247	0.086	0.330	0.173
EY-EZ -6	0.271	0.107	0.298	0.135	0.289	0.125	0.285	0.121

A precise framing for coupled instabilities is very important in order to choose a suitable design strategy. For weak and moderate interaction class, simple design methods based on safety coefficients can be used. In case of strong and very strong interaction, special design methods must be developed [14].

It can be observed that for the case of RSN125×3.2 pallet rack section, the computed erosion can classify the section into medium up to very strong interaction, depending on the considered imperfection.

4. CONCLUDING REMARKS

The main aim of this chapter was to provide evidences that the activity in the field of structural stability, particularly focussing the *mode interaction* problems, developed by the Timisoara researchers can be characterised as an activity of a *"school"*. Among the different subjects which have been subjects of theoretical, experimental and numerical investigation of the "*school"* in connection with that topic, those referring to *coupled bifurcations*, *erosion of critical bifurcation* load and *ultimate post-critical strength* are, in our opinion the most significant, leading to the so called *ECBL approach*, actually known as an available procedure enabling to calibrate buckling curves for mode interaction problems.

Received on July 16, 2014

REFERENCES

1. RONDAL, J., DUBINA, D., GIONCU, V. (guest editors), *Thin-walled Structures: Coupled Instabilities in Metal Structures*, Thin-walled Structures, **19**, *2–4*, and **20**, *1–4*, 1994.
2. RONDAL, J., DUBINA, D., GIONCU, V. (eds.), *Coupled Instabilities in Metal Structures - CIMS'96*, Imperial College Press, London 1996.
3. DUBINA, D., UNGUREANU, V. (eds.), Proceedings of the 6th International Conference on *Thin-Walled Structures: Recent Research Advances and Trends*, Volume 1 + 2, 5–7 September 2011, Timisoara, Romania, ECCS, 2011.
4. DUBINA, D., UNGUREANU, V. (guest editors), *Recent Research Advances on Thin-Walled Structures*, Special Issue, Thin-Walled Structures, **61**, December 2012.
5. DUBINA, D., IVANYI, M. (eds.), *Stability and Ductility of Steel Structures*, Proceedings of the 6th International Colloquium, First Session – SDSS'99, Timisoara, Romania, 9-11 September 1999, Elsevier Science Ltd., 1999.
6. RONDAL, J. (ed.), *Coupled Instabilities in Metal Structures. Theory and Practical Aspects*, CISM Courses and Lectures No. 379, Springer Verlag, Wien, New York, 1998.
7. RONDAL, J., DUBINA, D. (eds.), *Light gauge metal structures. Recent advances*, CIMS Udine Courses and Lectures – No. 455, Springer Verlag, Wien, New York, 2005.
8. PIGNATARO, M., GIONCU, V. (eds.), *Phenomenological and mathematical modelling of coupled instabilities*, CIMS Udine Courses and Lectures – No. 470, Springer Verlag, Wien, New York, 2005.
9. DUBINA, D. (guest editor), *Cold Formed Structures: Recent research advances in Central and Eastern Europe*, Special Issue, Thin-Walled Structures, **42**, *2*, 2004.
10. MATEESCU, D., GIONCU, V., DUBINA, D., *Timisoara Steel Structures Stability Research School: relevant contributions*, Journal of Constructional Steel Research. **55**, *1–3*, pp. 343–354, 2000.
11. DUBINA, D., UNGUREANU, V., *Review and Current Trends in Stability of Structures. Statics, Dynamics and Stability of Structures*, Vol. 3 (eds. K. Kowal-Michalska & R.J. Mania), Chapter 1: Mode interaction buckling in thin-walled bar members, pp. 19–68, TU Lodz Press, Poland, 2013.
12. GIONCU, V., BALUT, N., DUBINA, D., MOLDOVAN, A., PACOSTE, C., *Coupled instabilities in mono-symmetrical steel compression members*, Journal of Constructional Steel Research, **21**, *1–3*, pp. 71–95, 1992.
13. GIONCU, V., *General Theory of Coupled Instability*, Thin-Walled Structures, Special Issue on *Coupled Instability in Metal Structures*, **19**, *2–4*, pp. 81–128, 1994.
14. DUBINA, D., *The ECBL approach for interactive buckling of thin-walled steel members*, Steel & Composite Structures, **1**, *1*, pp. 75–96, 2001.
15. OLHOFF, N., SEYRANIAN, A.P., *Bifurcation and post-buckling analysis of bimodal optimum columns*, International Journal of Solids and Structures, **45**, pp. 3967–3995, 2008.
16. HUTCHINSON, J.W., KOITER, W.T., *Post-buckling theory*, Applied Mechanics Reviews, **23**, pp. 1353–1366, 1970.
17. THOMPSON, J.M.T., HUNT, G.W., *A General Theory of Elastic Stability*, Wiley, London, 1973.
18. THOMPSON, J.M.T., HUNT, G.W., *Elastic Instability Phenomena*, Wiley, London, 1984.
19. BUDIANSKY, B., *Theory of buckling and post-buckling behavior of elastic structures*, Advances in Applied Mechanics (ed. C.-S. Yih), **14**, pp. 1–65, 1974.
20. FLORES, F.G., GODOY, L.A., *Elastic post-buckling analysis via finite element and perturbation techniques. Part 1: Formulation*, International Journal of Numerical Methods in Engineering, **33**, pp. 1775–1794, 1992.
21. KOITER, W.T., *Current trends in the theory of buckling*, Proceedings of IUTAM Symposium. Buckling of Structures (ed. B. Budiansky), June 17–24, Cambridge, MA/USA, Springer, Berlin, pp. 1–16, 1976.
22. CHOW, C.-N., HALE, J.K., *Methods of Bifurcation Theory*, Grundlehren der Mathematischen Wissenschaften, **251**, Springer, New York, 1982.

23. GOLUBITSKY, M., SCHAEFFER, D., *Singularities and Groups in Bifurcation Theory*, Vol. I, Springer, New York, 1985.
24. GIONCU, V., IVAN, M., *Teoria comportarii critice si postcritice a structurilor elastic* (in Romanian), Edit. Academiei Romane, Bucharest, Romania, 1984.
25. KOITER, W.T., *On the stability of elastic equilibrium*, Thesis, Delft, English Translation, 1945, NASA TT-F10, 883 (1967) and AFFDL TR70-25 (1970).
26. BYSKOV, E., *Elastic buckling problem with infinitely many local modes*, Mechanics of Structures and Machines, **15**, *4*, pp. 413–435, 1987–1988.
27. Van der NEUT, A., *The interaction of local buckling and column failure of thin-walled compression members*, Proc. of the 12th Int. Congress on Applied Mechanics (eds. M.K. Heteny, W.G. Vincenti), Springer-Verlag, Berlin, 1969, pp. 389-399.
28. KOITER, W.T., KUIKEN, G.D.C., *The interaction between local buckling and overall buckling on the behavior of built-up columns*, Technical Report Rept. WTHD-23, Delft University of Technology, The Netherlands, 1971.
29. KOITER, W.T, *General Theory of Mode Interaction in Stiffened Plates and Shell Structures*, Technical Report Rept. WTHD-91, Delft University of Technology, The Nederland, 1976.
30. THOMPSON, J.M.T., LEWIS, G.M., *On the optimum design of thin walled compression members*, J. Mech. Phys. Solids, **20**, *2*, pp. 101–109, 1972.
31. TVEGAARD, V., *Imperfection-sensitivity of a wide integrally stiffened panel under compression*, International Journal of Solids and Structures, **9**, *1*, pp. 177–192, 1973.
32. TVEGAARD, V., *Influence of post buckling behavior on optimum design of stiffened panels*, International Journal of Solids and Structures, **9**, *12*, pp. 1519–1534, 1973.
33. RONDAL, J., MAQUOI, R., *Formulation d'Ayrton-Perry pour le flambement des barres métalliques*, Construction Métallique, **4**, pp. 41–53, 1979.
34. UNGUREANU, V., DUBINA, D., *Recent research advances on ECBL approach. Part I: Plastic-elastic interactive buckling of cold-formed steel sections*, Thin Walled Structures, **42**, *2*, pp. 177–194, 2004.
35. UNGUREANU, V., DUBINA, D., *Post-elastic strength and ductility of cold-formed steel sections*, Proc. of the Fourth International Conference on Thin-Walled Structures, Loughborough, UK, 22-24 June 2004, pp. 283–290.
36. SCHARDT, R., *Verallgemeinerte Technische Biegetheorie*, Springer-Verlag, Berlin, 1989.
37. DAVIES, J.M., LEACH, P., *First-order generalised beam theory*, Journal of Constructional Steel Research, **31**, *2–3*, pp. 187–220, 1994.
38. DAVIES, J.M., LEACH, P., HEINZ, D., *Second-order generalised beam theory*, Journal of Constructional Steel Research, **31**, *2–3*, pp. 221–241, 1994.
39. SILVESTRE, N., CAMOTIM, D., *First-order generalised beam theory for arbitrary orthotropic materials*, Thin-Walled Structures, **40**, *9*, pp. 755–789, 2002.
40. SILVESTRE, N., CAMOTIM, D., *Second-order generalised beam theory for arbitrary orthotropic materials*, Thin-Walled Structures, **40**, *9*, pp. 791–820, 2002.
41. SILVESTRE, N., CAMOTIM, D., *Nonlinear Generalized Beam Theory for Cold-formed Steel Members*, Int. Journal of Structural Stability and Dynamics, **3**, *4*, pp. 461–490, 2003.
42. CAMOTIM, D., DINIS, P.B., *Coupled instabilities with distortional buckling in cold-formed steel lipped channel columns*, Thin-Walled Structures, **49**, pp. 562–575, 2011.
43. SCHAFER, B.W., ÁDÁNY, S., *Buckling analysis of cold-formed steel members using CUFSM: Conventional and constrained finite strip methods*, Proc. of the 18th International Specialty Conference on Cold-Formed Steel Structures: Recent Research and Developments in Cold-Formed Steel Design and Construction, Orlando, Florida, October 2006. pp. 39–54.
44. LI, Z., SCHAFER, B.W., *Buckling analysis of cold-formed steel members with general boundary conditions using CUFSM: conventional and constrained finite strip methods*, Proc. of the Int. Specialty Conference on Cold-Formed Steel Structures, St. Louis, MO, November, 2010.

45. SCHAFER, B.W., *Designing cold-formed steel using the Direct Strength Method*, Proc. of the 18th International Specialty Conference on Cold-Formed Steel Structures, October 26-27, Orlando, Florida, USA, 2006.
46. *** *Supplement 2004 to the North American Specification for the Design of Cold-Formed Steel Structural Members*, 2001, Edition: *Appendix 1 – Design of Cold-Formed Steel Structural Members Using Direct Strength Method*. American Iron and Steel Institute, Washington, D.C., SG05-1, 2004.
47. GARCEA, G., MADEO, A., ZAGARI, G., CASCIARO, R., *Asymptotic post-buckling FEM analysis using corotational formulation*, Int. J. Solids and Structures, **49**, pp. 377–397, 2009.
48. GARCEA, G., MANDEO, A., CASCIARO, R., *The implicit corotational method and its use in the derivation of nonlinear structural models for beams and plates*, Journal of Mechanics of Materials and Structures, **7**, *6*, pp. 509-538, 2012.
49. HEMP, W.S., *The Theory of Flat Panels Buckled in Compression*, Reports and Memoranda, Aeronautical Research Council, No. 2178, 1945.
50. van der NEUT, A., *The Sensitivity of Thin-walled Compression Members to Column Axis Imperfection*, Int. Journal of Solids and Structures, **9**, pp. 999–1011, 1973.
51. GEORGESCU, M., *Instability problems by Thin-walled Cold-formed Steel Members*, "Politehnica" University of Timisoara, PhD Thesis, 1998.
52. DUBINA, D., UNGUREANU, V., *Lateral-Torsional and Local Interactive Buckling of Thin-Walled Cold-Formed Beams*, Rev. Roum. Sci. Techn. – Méc. Appl., **42**, *5–6*, pp. 467–481, 1997.
53. DUBINA, D., UNGUREANU, V., *Effect of imperfections on numerical simulation of instability behaviour of cold-formed steel members*, Thin Walled Structures, **40**, *3*, pp. 239–262, 2002.
54. CRISAN, A., UNGUREANU, V., DUBINA, D., *Behaviour of cold-formed steel perforated sections in compression. Part 1 – Experimental investigations*, Thin Walled Structures, **61**, pp. 86–96, 2012.
55. CRISAN, A., UNGUREANU, V., DUBINA, D., *Behaviour of cold-formed steel perforated sections in compression. Part 2 – Numerical investigations and design considerations*, Thin Walled Structures, **61**, pp. 97–105, 2012.
56. DUBINA, D., UNGUREANU, V., CRISAN, A., *Experimental Evidence of Erosion of Critical Load in Interactive Buckling*, Journal of Structural Engineering – ASCE, **139**, *5*, pp. 705–716, 2013.
57. UNGUREANU, V., DUBINA, D., *Sensitivity to Imperfections of Perforated Pallet Rack Sections*, Mechanics and Mechanical Engineering, **17**, *2*, 209–222, 2013.
58. UNGUREANU, V., KOTEŁKO, M., MANIA, R.J., DUBINA, D., *Plastic mechanisms database for thin-walled cold-formed steel members in compression and bending*, Thin Walled Structures, **48**, *10–11*, pp. 818–826, 2010.
59. DUBINA, D., UNGUREANU, V., *Instability mode interaction: From Van Der Neut model to ECBL approach*. Thin-Walled Structures, **81**, AS4100-1990, pp. 39–49, 2014.
60. *** *Australian Standard: Steel Structures*, Homebush, Australia, 1990.